

Enhancement of EAST plasma control capabilities



Bingjia Xiao^{a,b,*}, Qiping Yuan^a, Zhengping Luo^a, Yao Huang^a, Lei Liu^a, Yong Guo^a, Xiaofang Pei^a, Shuliang Chen^a, D.A. Humphreys^c, A.W. Hyatt^c, Dennis Mueller^d, G. Calabró^e, F. Crisanti^e, R. Albanese^f, R. Ambrosino^f

^a Institute of Plasma Physics, Chinese Academy of Sciences, Hefei, China

^b School of Nuclear Science and Technology, University of Science and Technology of China, Hefei, China

^c General Atomics, P.O. Box 85608, San Diego, CA 92186-5608, United States

^d Princeton Plasma Physics Laboratory, Princeton, NJ, United States

^e ENEA Unità Tecnica Fusione, C.R. Frascati, Via E. Fermi 45, 00044 Frascati, Roma, Italy

^f CREATE, Università di Napoli Federico II, Università di Cassino and Università di Napoli Parthenope, Via Claudio 19, 80125 Napoli, Italy

HIGHLIGHTS

- Parallel plasma equilibrium reconstruction using GPU for real-time control on EAST.
- Vertical control using Bang-bang + PID method to improve the response and minimize the oscillation caused by the latency.
- Quasi-snowflake divertor plasma configuration has been demonstrated on EAST.

ARTICLE INFO

Article history:

Received 20 June 2015

Received in revised form 19 May 2016

Accepted 2 June 2016

Available online 18 June 2016

Keywords:

EAST

PEFIT

Quasi-snowflake

Vertical control

ABSTRACT

In order to improve the plasma control performance and enhance the capability for advanced plasma control, new algorithms such as PEFIT/ISOFLUX plasma shape feedback control, quasi-snowflake plasma shape development and vertical control under new vertical control power supply, have been implemented and experimentally tested and verified in EAST 2014 campaign. P-EFIT is a rewritten version of EFIT aiming at fast real-time equilibrium reconstruction by using GPU for parallelized computation. Successful control using PEFIT/ISOFLUX was established in dedicated experiment. Snowfldivertor plasma shape has the advantage of spreading heat over the divertor target and a quasi-snowflake (QSF) configuration was achieved in discharges with $I_p = 0.25$ MA and $B_t = 1.8$ T, $\kappa \sim 1.9$, by plasma position feedback control. The shape feedback control to achieve QSF shape has been preliminary implemented by using PEFIT and the initial experimental test has been done. For more robust vertical instability control, the inner coil (IC) and its power supply have been upgraded. A new control algorithm with the combination of Bang-bang and PID controllers has been developed. It is shown that new vertical control power supply together with the new control algorithms results in higher vertical controllability.

© 2016 Elsevier B.V. All rights reserved.

1. Introduction

In 2014 EAST campaign, we worked on (1) PEFIT/ISOFLUX plasma shape feedback control, (2) quasi-snowflake plasma shape development, and (3) vertical control under new inside coil (IC) position and new power supply to improve the plasma control performance and enhance the capability for advanced plasma control.

An essential requirement for optimum performance of a tokamak discharge is accurate feedback control of many of the discharge parameters. Many of these discharge parameters, such as shape and safety factor profile can be evaluated from magnetic diagnostic data [1–3]. In Ref. [4], a real-time version of EFIT called rEFIT has been developed for the real-time shape feedback control. RtEFIT used the fast loop which contains a least square fit to the plasma current model and then generates control errors directly from these fitted current sources. A full loop equilibrium solver (slow loop) can only be finished after several fast loops. In order to speed-up the full loop equilibrium reconstruction, a parallel code named PEFIT [5] has been implemented on multiple GPU's (Graphical Processing Unit). PEFIT can complete one full equilibrium reconstruction iter-

* Corresponding author at: Institute of Plasma Physics, Chinese Academy of Sciences, Hefei, China.

E-mail address: bjxiao@ipp.ac.cn (B. Xiao).

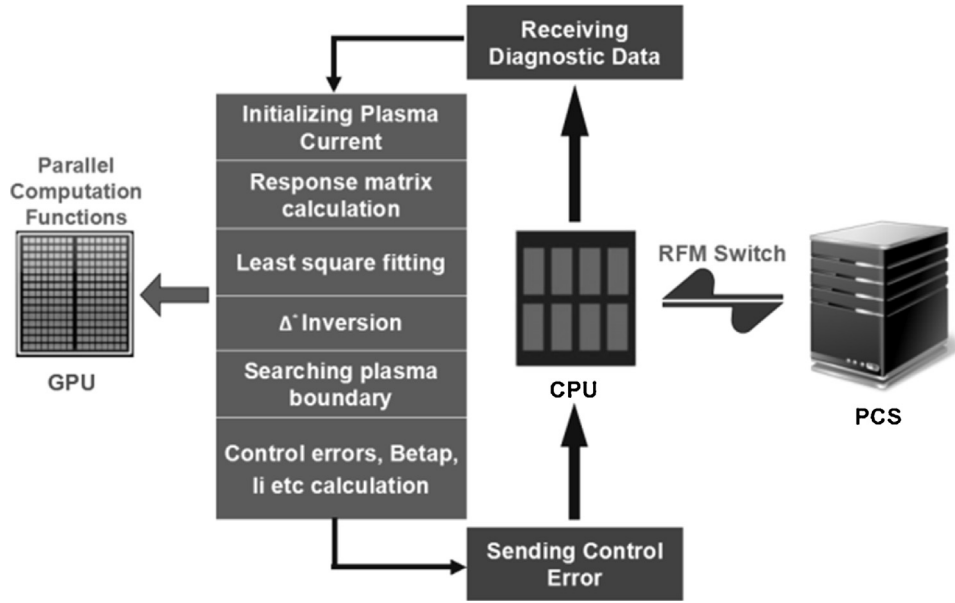


Fig. 1. PEFIT flow chart: optimization of GPU/CPU interactions.

Table 1
Upgraded vs PS parameters.

Maximum current	10 kA (6 kA limited in 2014)
Maximum voltage	1600 V
Total delay and rise time	0.5 ms

ation on even finer grids within a period about 300 micro-seconds which is comparable with an rtEFIT fast loop cost. Results from EAST and DIII-D single static equilibrium benchmark tests indicate that P-EFIT can accurately reproduce the EFIT reconstruction algorithms at a fraction of the computation time. Simulated testing using the EAST plasma control model implemented in the PCS, show similar PEFIT and rtEFIT control errors when operating on real EAST discharge data. Successful control using ISOFLUX/P-EFIT was established in the dedicated experiment during the EAST 2014 campaign. This implementation and experimental verification is described in Section 2.

Reduction of heat loads on the divertor plates is one of the most challenging issues for a tokamak reactor. Many solutions have been proposed. Among them, one idea is to use geometrical effect for a stronger flaring of poloidal field in the divertor [6]. Snowflake divertor (SFD) configuration is one example of this concept [7–9]. During 2014 campaign, first quasi-snowflake (QSF) divertor configuration was demonstrated on EAST. In Section 3, we summarize the first appearance of EAST QSF divertor shape and its influence on the head load.

For the vertical instability control, the inner coil (IC) and its power supply have been upgraded. The new IC power supply can be operated based on voltage mode or current mode. A new control algorithm with the combination of Bang-bang and PID controllers has been developed using voltage mode. In Section 4, we will report briefly the features of the new power supply and the new vertical control method and the enhancement to the vertical controllability. The detailed discussion about the control method can be found in [17].

2. PEFIT/ISOFLUX plasma shape control

PEFIT is based on the EFIT framework described in [1–3], but takes advantage of massively parallel Graphical Processing

Unit (GPU) cores to significantly accelerate the computation. It is built with the CUDA™ architecture to optimize the middle-scale matrix multiplication and the algorithm which solves block tri-diagonal linear system efficiently in parallel by using GPU. As shown in Fig. 1, the major time-consuming computing parts of EFIT's algorithm are: poloidal flux refreshing (Δ^* Inversion), response matrix calculation and least square fitting. Equation (1) shows the poloidal flux refreshing (Δ^* Inversion), which calculate the flux on grid points after getting the plasma current distribution.

$$\Delta^* \psi = -\mu_0 R J_\phi, \quad J_\phi = RP'(\psi) + \frac{\mu_0 FF'(\psi)}{4\pi^2 R} \quad (1)$$

As is done in EFIT, finite difference method is used and the partial differential equation transformed into a block tri-diagonal equation set. By eigenvalue decomposition, the block tri-diagonal equation is transformed into independent triangular system that could be solved in parallel on GPU.

A set of the magnetic measurement M_i , such as poloidal field and flux sensors located at position r_i surround the plasma circumference, can be expressed as the linear summation of current source contributions, (coils, current carrying structures and plasma) as:

$$C_i(r_i) = \sum_{n=1}^{n_c} G_{C_i}(r_i, r_n) I_e^{(n)} + \iint_A G_{C_i}(r_i, r') J dr' dZ' \quad (2)$$

where G is the green functions which is only depend on the geometry factors of the sensor and the current. The second term is the integration over the entire plasma cross section A . The control errors in the ISOFLUX algorithms can be expressions in a form similar to Eq. (2). Thus the control error calculation is mainly consisted of two large matrix multiplications if current sources or their expressions are known. By dividing the matrix into small parts which can be solved by different GPU cores, the overall time of matrix elements multiplications, additions and data accessing can be reduced.

The plasma current parameters and external coil currents are solved by minimizing,

$$\chi^2 = \sum_{i=1}^{n_M} \left(\frac{M_i - C_i}{\sigma_i} \right)^2 \quad (3)$$

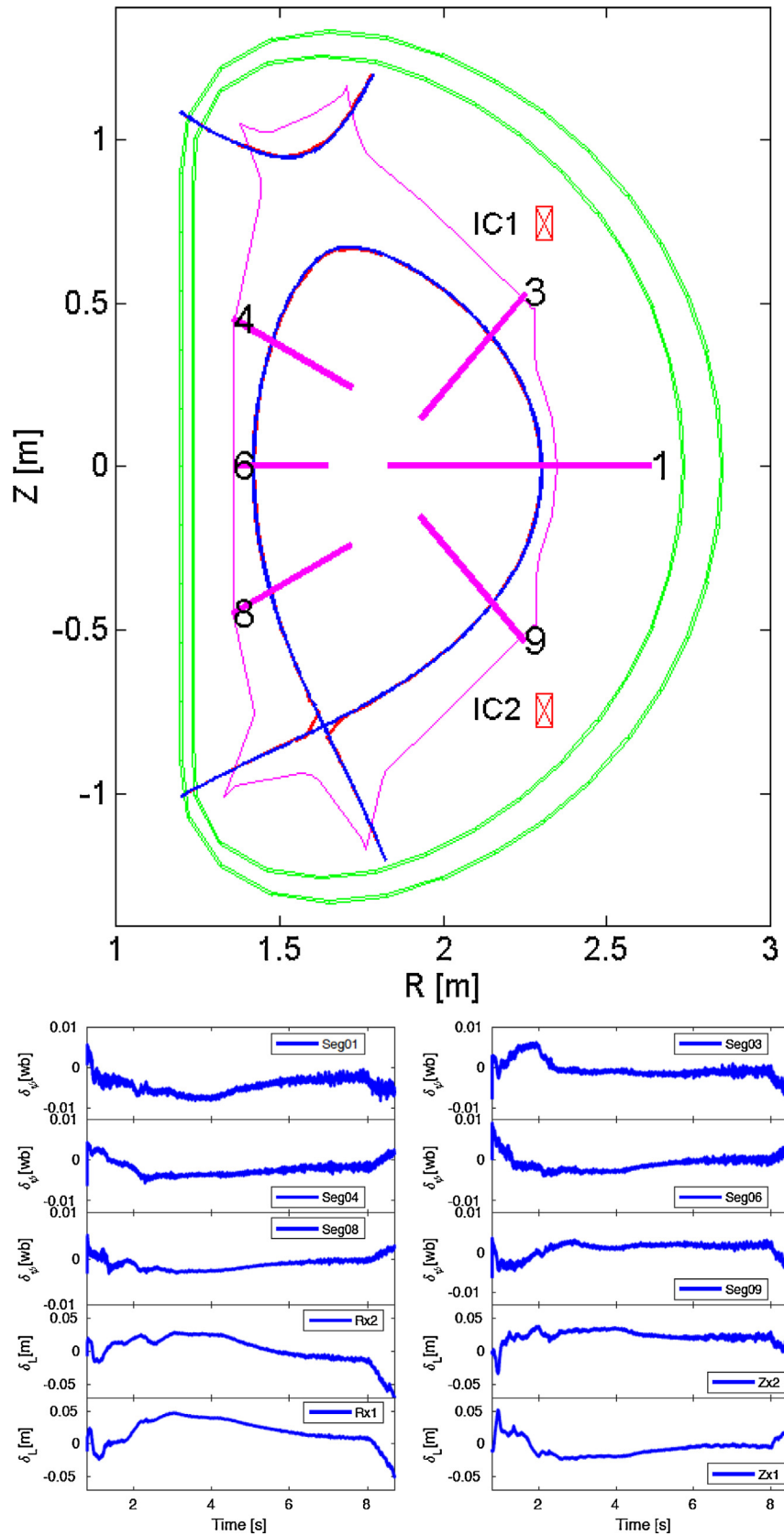


Fig. 2. Shot 51044 was controlled by PEFIT/ISOFLUX. The top frame: the boundary result comparison between PEFIT (red line) and EFIT (blue line) at 4.78 s and the control segments (pink line). Bottoms 10 frames: the control errors on all the segments and 2 X points (for interpretation of the references to colour in this figure legend, the reader is referred to the web version of this article.)

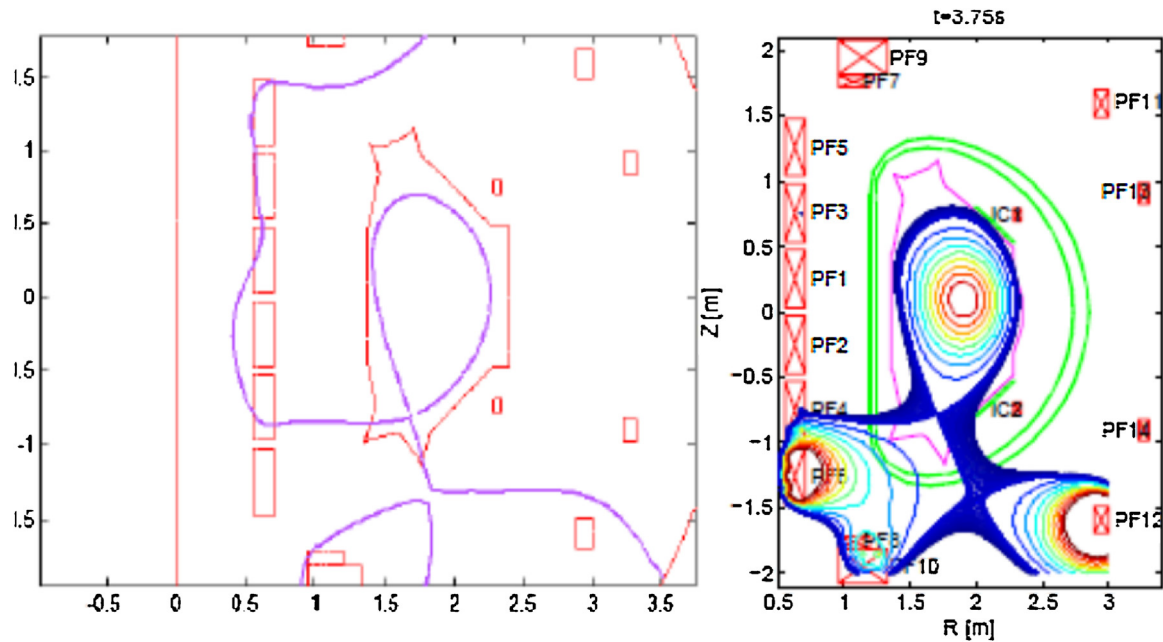


Fig. 3. The target configuration for EAST QSF experiment (left) and EFIT constructed equilibrium for shot 47660 at 3.75 s (right).

EFIT solves this equation by singular-value decomposition. PEFIT makes use of parallel matrix multiplication, the initial over-determined equation system is transformed into full rank system and can be solved directly.

Although PEFIT could obtain a well-converged equilibrium result with sufficient accuracy in 8–9 iterations in about 2.5 ms which is more than ten times faster than EFIT, it still can not satisfy the requirement of real-time control in EAST tokamak operation. For this reason, a strategy similar to rtEFIT is adopted [4]. The procedure is to use the equilibrium result at last time-slice as the initial solution for the next time step and at each time step only 1 or 2 iterations are performed. For each iteration, the most recent diagnostic data are used. With this treatment, PEFIT can meet both the accuracy and real-time needs for EAST plasma shape feedback control on a 65×65 spatial grid. EAST PCS [10,11] is a linux cluster configured with several real-time control computer nodes linked with low latency MYRINET network. RFM has been successfully applied in the system for data connection between PCS and tokamak systems such as power supply and real-time data acquisitions. For PEFIT calculation, we adopt also the RFM for the data communication between GPU computer and PCS. The flow chart of PEFIT and its communication with EAST PCS is shown in Fig. 1.

Simulated testing has been conducted using the EAST plasma control model implemented in PCS with input based on EAST real discharge shot data. Details of the simulation and benchmark accuracy and validation can be found in [16]. It was shown that the PEFIT reconstruction agrees well with EFIT result with the full single loop iteration time comparable with that is used by a rtEFIT fast loop. In dedicated experiment during the EAST 2014 campaign, we replaced rtEFIT with PEFIT to control the plasma shape. Fig. 2 shows the control results using PEFIT/ISOFLUX algorithm for shot 51044. The PEFIT reconstruction in most of the time slices agrees well with EFIT. The top frame of Fig. 2 shows the comparison of the reconstructed plasma boundary at a typical time slice. The bottom frame of Fig. 2 shows the control errors evolution of this shot. The control is stable and reliable and it is proven that current version of PEFIT can be used in the real-time shape feedback control for EAST plasma.

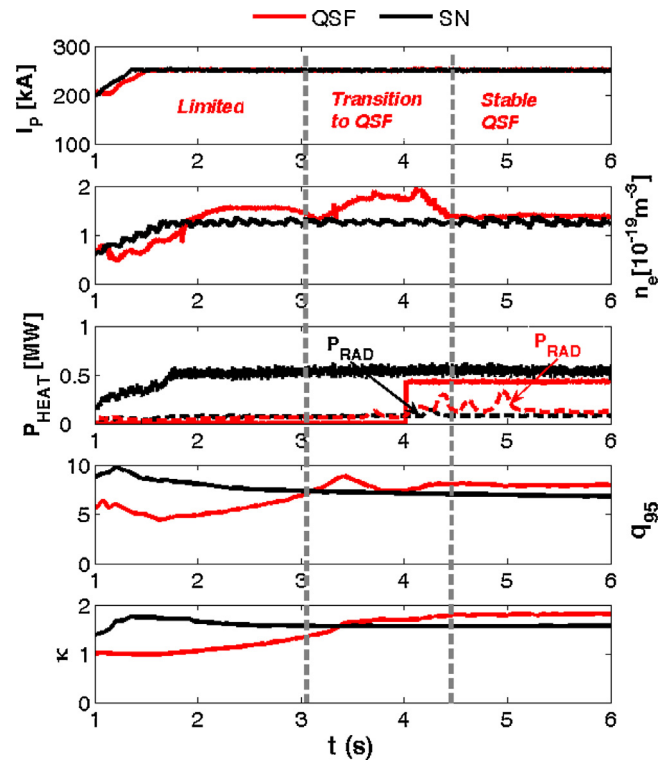


Fig. 4. Time evolution of main plasma quantities for LSN (#47038, black line) and QSF (#48971, red line) (for interpretation of the references to colour in this figure legend, the reader is referred to the web version of this article.)

3. Quasi-snowflake plasma shape

In 2014 experimental campaign, we performed experiment with SFD configuration. Unlike NSTX and DIII-D, EAST does not have specific divertor coils to independently shape the snowflake in the divertor region. Unlike TCV, EAST only has 12 independent PF coils and a smaller divertor vacuum region to shape plasma. Generations of a standard SFD configuration is difficult for EAST. One Quasi-SFD

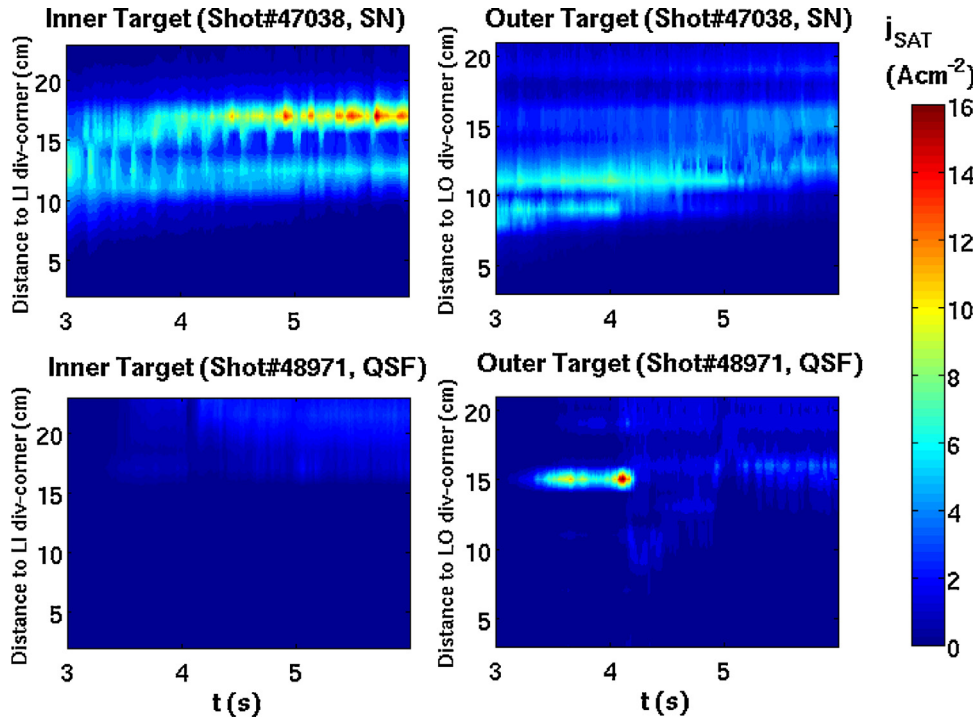


Fig. 5. Spatial-temporal profile of ion saturation current density for LSN (#47038, upper two figures) and QSF (#48971, lower two figure) discharges.

configuration, shown as Fig. 3 (left frame), can be achieved in east with PF currents limited to 10 kA/turn. This was the primary target for the 2014 campaign. In experiment, the plasma current is ramped up to 250 kA at 1.5 s with circular limiter configuration. Then, the plasma evolves to target QSF configuration from 1.6 s to 3.75 s by position and current control. The preprogrammed feed-forward PF currents at 3.75 s are carefully set to form the poloidal flux distribution in the divertor region. Shot 47660 is one such shot, which achieved the QSF configuration at 3.75, and keep the QSF configuration to 5.25 s. The reconstructed equilibrium by EFIT at 3.75 s is shown as Fig. 3 (right frame).

Because these experiments focused only on the control issues to achieve the QSF configuration, we did not do dedicated experiment for a comparison of heat load. Here we only do a simple comparison between QSF and lower single null (LSN). Shot 48971 is QSF experiment with NBI injected at 4 s, for the comparison we selected shot 47038 in LSN configuration with most similar plasma and heating conditions with shot 48971. We notice that the heating source @ 47038 is LHW but the effective heating power is even less than that @ 48971 because the heating efficiency of NBI is higher than LHW. The plasma quantities are similar after 4.5 s, shown as Fig. 4. Divertor probes give the spatial-temporal profile of ion saturation current density j_{SAT} for these two shots, shown as Fig. 5. j_{SAT} is stable for LSN discharge. For QSF discharge, j_{SAT} at the outer target significantly decreases after 4.5 s when the QSF configuration is formed. It indicates QSF could reduce the heat flux on the divertor. The infrared camera measurements also prove it, shown as Fig. 6. Because (1) the plasma parameters are relative small which causes the quality of diagnostic data is not well, and (2) the plasma parameters of the LSN and QSF discharges are not same, quantitative analysis requires further experiments.

4. Upgraded vertical control

The vertical control for EAST was marginal before 2012 and the maximum controllable vertical disturbance is only 1.2 cm in normal 400 kA discharge with reasonable growth rate plasmas [14]. For

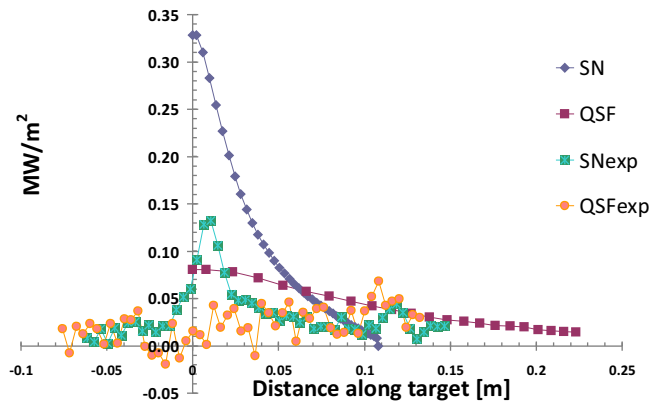


Fig. 6. Infrared camera measurement (SNexp and QSFexp) and simulated power density (SN and QSF) at the outer target.

the 2014 campaign, the inside coil (IC) position was modified for better vertical control and its power supply (VS PS) was upgraded to provide higher current and voltage, faster response and voltage control capability. The new power supply parameters are shown in Table 1.

The improvements in the IC location and power supply have allowed stabilization of high growth rate plasmas, like the QSF configuration, during the 2014 campaign. When compared to the old IC power supply, the new voltage control mode has greatly improved the controllability of high vertical growth rate plasmas.

A Bangbang controller (time optimal control) has been developed for EAST vertical control. The RZIP rigid plasma response model [12,13] has been used to design the Bangbang controller. This model can be expressed in the standard state-space model form,

$$\begin{cases} \dot{X} = Ax + Bu \\ y = Cx + Du \end{cases} \quad (4)$$

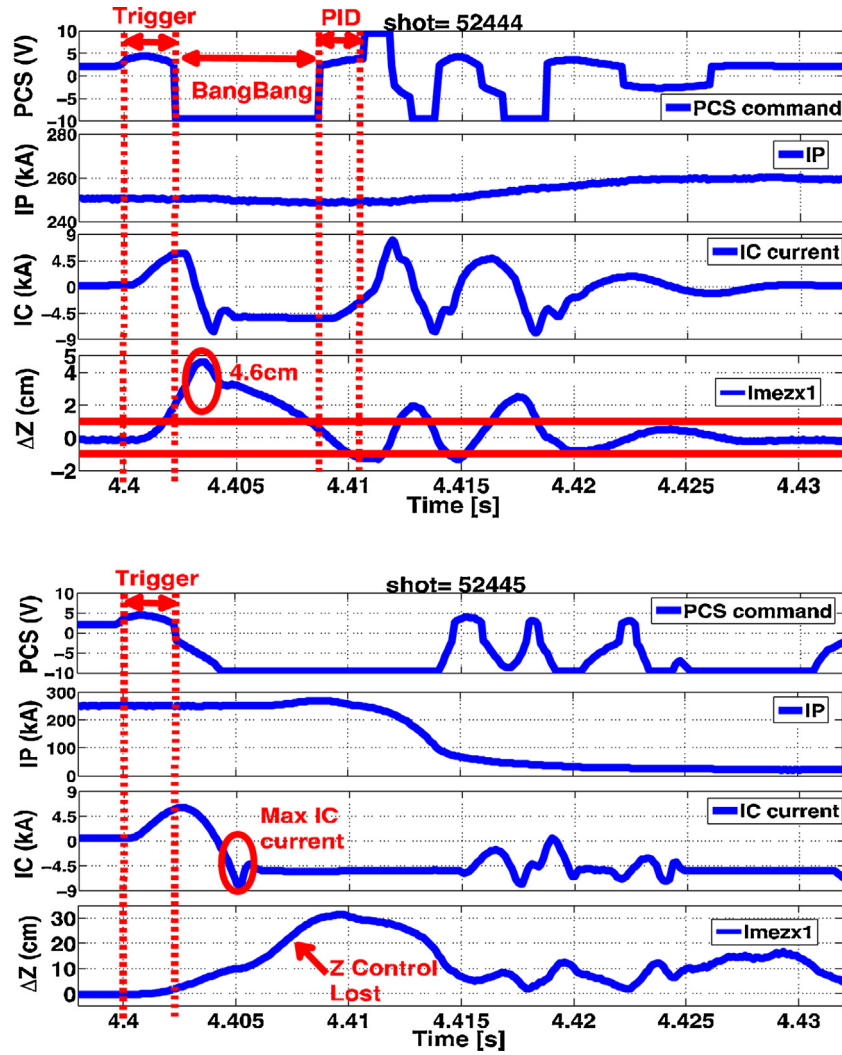


Fig. 7. The comparison between combined Bangbang controller (#52444) and PID controller(#52445).

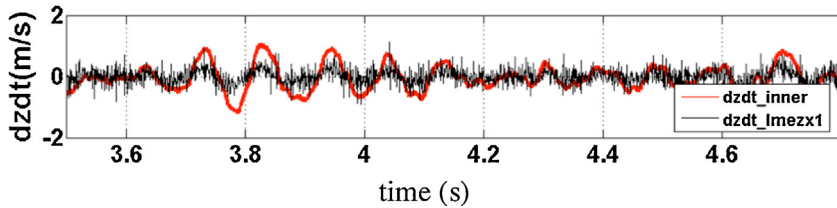


Fig. 8. Shot 49422, the comparison of dz/dt calculated by loop voltage (red) and lmsz signal (black). (For interpretation of the references to colour in this figure legend, the reader is referred to the web version of this article.)

where the matrix D is ignored in the analysis. Y can be further rewritten as,

$$\dot{y} = CAC^{-1} \times y + CBu \quad (5)$$

For the vertical displacement response, it can be given by

$$\dot{Z} = \gamma_z Z + CBu_{ic} \quad (6)$$

where the parameter γ_z is the maximum eigenvalue of the matrix CAC^{-1} . By using the minimum principle, the time optimal control law is given by

$$u^*(t) = V_{max} \times \text{sgn}(Z_{error}) \quad (7)$$

where the parameter V_{max} is the maximum output voltage of the IC power supply.

In addition, the time delay of the control system T_{ps} must be included in EAST vertical displacement control system. In a Bangbang controller this time delay will cause an oscillation about the target. With the introduction of a time delay, we combined the Bangbang controller with a PID controller and the optimal control law is given by

$$u(t) = \begin{cases} V_{max} \times \text{sgn}(Z_{error} + K \times \frac{dz}{dt}), & \text{if } |Z_{error}| > Z_{lim} \\ K_p \times Z_{error} + K_d \times \frac{dz}{dt}, & \text{if } |Z_{error}| \leq Z_{lim} \end{cases} \quad (8),$$

where the parameters K and Z_{lim} are related to T_{ps} .

To apply this control algorithm and test the vertical controllability, we used the quasi-snowflake shape for the test. The selected

shape in shot 52444 at 4.4 s has the free drift vertical growth rate about 500/s which is much higher than normal EAST divertor discharge. The vertical control was turned off at 4.4 s and moreover, we applied 500 V IC voltage for 4 ms to trigger a VDE (Vertical Displacement Event). After vertical displacement grew to certain level, the vertical controller was turned on. While $|Z_{\text{error}}| > 1\text{cm}$, the Bangbang controller is activated and output the maximum voltage. When $|Z_{\text{error}}| \leq 1\text{cm}$, the controller switches to the PID control. The result of this shot show the combined Bangbang & PID controller can successfully recover the vertical position with disturbances of dz as high as 4.6 cm. This compares with a much lower $dZ_{\text{max}} = 1.2\text{cm}$ controlled by PID and IC current control in 2012 [14]. As a comparison, shot 52445 repeated the shot 52444, but used only PID controller. The vertical control was lost, as shown in Fig. 7. The Bangbang + PID controller results in quick response of vertical control in large vertical disturbance and quiet oscillation when the disturbance is small.

The signal to noise ratio is always an issue for a vertical stabilization in elongated divertor plasma. In routine EAST experiment, the vertical plasma current center (Z_c) is estimated by a set of magnetic sensors for poloidal field measurement. This introduces integrator noise. For stabilizing vertical motion, control of the vertical displacement rate, dz/dt , is more important than overall position control z . Direct dz/dt control using differential loop voltage signals is suggested in [15] and was tested in the 2014 EAST campaign.

During a vertical motion of plasma, the measured flux loop voltage is

$$V = -\frac{d\psi}{dt} = -\frac{d(M_{\text{pl}} \times I_p)}{dt} = -\left(I_p \frac{\delta M_{\text{pl}}}{\delta t} + M_{\text{pl}} \frac{\delta I_p}{\delta t}\right) \quad (9)$$

Here, M_{pl} is the mutual inductance between the plasma and flux loops, I_p is the plasma current. For small z position oscillation, we can assume the plasma current remains constant, i.e. $\delta I_p / \delta t = 0$. The difference of two loop voltages is

$$V_1 - V_2 = \left(\frac{\delta M_{\text{p2}}}{\delta t} - \frac{\delta M_{\text{p1}}}{\delta t}\right) I_p = \left(\frac{\delta M_{\text{p2}}}{\delta z} - \frac{\delta M_{\text{p1}}}{\delta z}\right) \frac{\delta z}{\delta t} I_p \quad (10)$$

Rearranging the terms:

$$\frac{\delta z}{\delta t} = \frac{V_1 - V_2}{I_p} \times \frac{1}{\left(\frac{\delta M_{\text{p2}}}{\delta z} - \frac{\delta M_{\text{p1}}}{\delta z}\right)} = C \times \frac{V_1 - V_2}{I_p} \quad (11)$$

Fig. 8 shows the dz/dt calculated by loop voltage for shot 49422. Comparing with $d(lmsz)/dt$, where $lmsz$ is the PCS predicted location of the plasma from magnetic measurements, the noise ratio has been greatly improved. This means we could get the plasma vertical velocity in higher S/N ratio from a set of loop voltages. In future experiment, we will apply dz/dt calculation for the vertical control.

5. Summary

In EAST 2014 campaign, PEFIT finished one-iteration calculation in 0.3 ms for 65×65 grid, and PEFIT/ISOFLUX has been used for EAST plasma shape control. It would be used for the further plasma profile control. QSF configuration with $I_p = 250\text{KA}$ has been achieved by RZ I_p control. In the following campaigns, shape feedback control will be used to systematically explore the controllability of QSF plasma shapes and their influence on the reduction of the divertor heat load. With the upgraded IC power supply, combined Bangbang & PIC control method has been developed. More robust vertical control has been achieved.

Acknowledgments

This work is supported the National Magnetic Confinement Fusion Research Program of China under Grant No. 2014GB103000, and the National Natural Science Foundation of China under Grant No. 11305216 and No. 11205191.

References

- [1] L.L. Lao, et al., Nucl. Fusion 25 (1985) 1611.
- [2] L.L. Lao, et al., Fusion Sci Technol. 48 (2005) 968.
- [3] L.L. Lao, et al., Nucl. Fusion 30 (1990) 1035.
- [4] J.R. Ferron, et al., Nucl. Fusion 38 (1998) 1055.
- [5] X.N. Yue, et al., Plasma Phys. Controlled Fusion 55 (2013) 085016.
- [6] D.D. Ryutov, Phys. Plasma 14 (2007) 064502.
- [7] F. Piras, et al., Plasma Phys. Controlled Fusion 52 (2010) 124010.
- [8] V.A. Soukhanovskii, et al., J. Nucl. Mater. 415 (2011) S365.
- [9] Y. Guo, et al., JPS Conf. Proc. 1 (2014) 015035.
- [10] B.J. Xiao, et al., Fusion Eng. Des. 87 (2012) 1887–1890.
- [11] Q.P. Yuan, et al., Nucl. Fusion 53 (2013) 043009.
- [12] D.A. Humphreys, et al., Bull. Am. Phys. Soc. 44 (1999) 175–182.
- [13] D.A. Humphreys, et al., Nucl. Fusion 49 (2009) 115003.
- [14] L. Liu, et al., Fusion Eng. Des. 89 (2014) 563–567.
- [15] S.P. Gerhardt, et al., Sci. Instrum. 85 (2014) 11E807.
- [16] Y. Huang, et al., Fusion Eng. Des., In Press, Available online May 2016.
- [17] Y.H. Wang, B.J. Xiao, L. Liu, Q.P. Yuan, Fusion Eng. Des., In Press, Available online May 2016.